

See discussions, stats, and author profiles for this publication at: <https://www.researchgate.net/publication/280536329>

Anaerobic Degradation Pathway of the Novel Chiral Insecticide Paichongding and Its Impact on Bacterial Communities in Soils

ARTICLE in JOURNAL OF AGRICULTURAL AND FOOD CHEMISTRY · JULY 2015

Impact Factor: 2.91 · DOI: 10.1021/acs.jafc.5b02645 · Source: PubMed

CITATIONS

3

READS

28

6 AUTHORS, INCLUDING:



Zhiqiang Cai

Changzhou University

23 PUBLICATIONS 77 CITATIONS

SEE PROFILE

Anaerobic Degradation Pathway of the Novel Chiral Insecticide Paichongding and Its Impact on Bacterial Communities in Soils

Zhiqiang Cai,* Jing Wang, Jiangtao Ma, Xiaolin Zhu, Jinyan Cai, and Guanghua Yang*

Laboratory of Applied Microbiology, School of Pharmaceutical Engineering & Life Science, Changzhou University, Changzhou 213164, China

ABSTRACT: To comprehensively understand anaerobic degradation of the novel *cis*-nitromethylene neonicotinoid insecticide Paichongding (IPP) and its impacts on microbial communities in anaerobic soils, we investigated IPP degradation characteristics, kinetics, and pathway in four different soils. The bacterial community in response to the application of IPP using pyrosequencing of 16S rRNA gene amplicons was also studied. The removal ratio of IPP stereoisomers (RR-IPP, SS-IPP, RS-IPP, and SR-IPP) reached >90% at 60 days after IPP treatment (DAT) in yellow loam soil (F) and paddy field on desalting muddy polder (C), whereas the degradation ratios of RR-IPP and SS-IPP were <30% at 60 DAT in Huangshi soil (J) and yellow paddy soil (H). The results showed that the anaerobic degradation rate of IPP and its stereoisomers was strongly affected by soil physical–chemical characteristics. Furthermore, on the basis of the six metabolites (M1–M6) identified by LC-MS/MS and their behavior, the anaerobic degradation pathway of IPP in soils was proposed. Biodegradation of IPP involved continuous biocatalytic reactions such as nitro reduction and elimination, hydrolysis, demethyl, and ether cleavage reactions. A higher richness of operational taxonomic units (OTUs) was found in soils without IPP application than in soils with IPP application. Both the rarefaction curves and Shannon–Wiener diversity index in anaerobic soils had significant difference after IPP application, and the community composition also differed at both the phyla and genus levels.

KEYWORDS: IPP, degradation pathway, anaerobic degradation, soil bacterial community, bacterial diversity

INTRODUCTION

Chiral insecticides have been widely used in modern agricultural systems to ensure good harvests; they currently constitute about 25% of all pesticides used, and this ratio is increasing as more complex structures are introduced.¹ Chiral compounds often have two or more stereoisomers, which have similar physicochemical properties, but there are significant differences between the enantiomers in biological activity, toxicity, toxicology, absorption transfer, and metabolism in the natural environment.^{1–4} Such stereoisomer effects have been reported for pyrethroids, acetanilides, organophosphorus pesticides, and other pesticides over the past three decades.^{2–4}

Paichongding (IPP; 1-((6-chloropyridin-3-yl)methyl)-7-methyl-8-nitro-5-propoxy-1,2,3,5,6,7-hexahydroimidazo[1,2- α]-pyridine), is a novel chiral insecticide recently developed by East China University of Science and Technology in China.^{4–9} It has two chiral carbon centers, which leads to four stereoisomers (RR-IPP, SS-IPP, RS-IPP, and SR-IPP; Figure 1). IPP has excellent toxicity toward a broad spectrum of sucking and biting insects.^{10–12} Traditional neonicotinoid insecticides are selective agonists of the insect nicotinic acetylcholine receptors (nAChRs); IPP is a novel neonicotinoid as it is the antagonist of nAChRs of insects.^{4–7} In addition, IPP activity is about 40–50 times higher than that of imidacloprid against imidacloprid-resistant insects.^{13–19} A 10% IPP suspension concentration has been permitted to be used in China.^{7,8,12} The wide application of IPP also could accumulate inactive isomers in the environment, which may do harm to ecosystems and crop productivity. Insecticide-resistant insects may also result. The transformation and behavior of IPP in the environment are important requirements for its safe on food crops,^{5–8} and the large

amount of insecticide application can also affect the soil microbial community by changing their number and enzyme activity.^{9–13} Several reports have mainly focused on its photodegradation in aqueous solution, translocation in Youdonger (Chinese cabbage), stereoselective fate in flooded soils and its metabolism, extractable and bound residue, and transformation in soils.^{4–8,14,15,17} Enantioselective degradation kinetics and behavior of IPP, its degradation pathway, and the effect of IPP on soil microbial communities in anaerobic soils have not been reported until now. The main objective of this research was to investigate the enantioselective kinetics of IPP in anaerobic soils and its effect on soil microbial community and diversity; the results would provide more data for better understanding the degradation kinetics and behavior of IPP in the environment and evaluating food safety at the level of enantiomers.

MATERIALS AND METHODS

Chemicals and Test Soils. Paichongding (IPP; 10% IPP suspension concentration) was obtained from Jiangsu Kesheng Co. Ltd., and HPLC grade methanol and acetonitrile were purchased from Burdick & Jackson (Muskegon, MI, USA). All other reagents and common chemicals were of analytical grade and purchased from Sinopharm Chemical Reagent Co. (Shanghai, China).

Four different types of soil from different agricultural fields were used in this study; they were yellow loam soil (F, GB/T-A2111411, Fujian province), Huangshi soil (J, GB/T-G2511211, Jiangsu province), paddy field on desalting muddy polder (C, GB/T-H2121315, Cixi, Zhejiang

Received: May 28, 2015

Revised: July 23, 2015

Accepted: July 27, 2015

Published: July 27, 2015

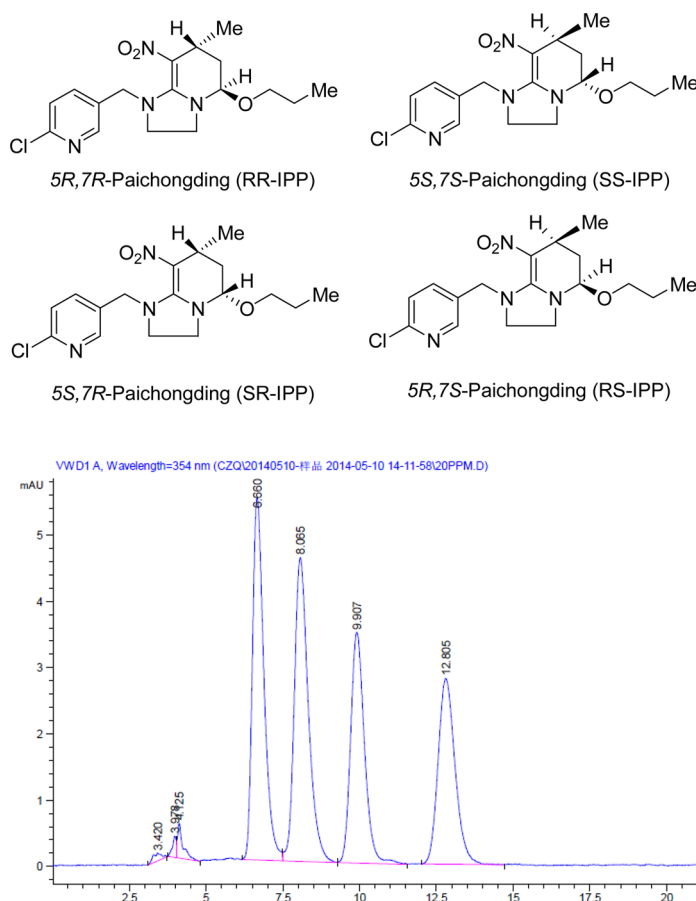


Figure 1. Stereostructures of four isomers of Paichongding (IPP) and HPLC chromatograms of IPP. Peaks 1, 2, 3, and 4 represent stereoisomers RR-IPP, SS-IPP, SR-IPP, and RS-IPP, respectively.

Table 1. Physicochemical Characteristics of the Experimental Soils

characteristic	yellow loam soil (F)	Huangshi soil (J)	paddy field on desalting muddy polder (C)	yellow paddy soil (H)
location	Longquan, Fujian province	Changzhou, Jiangsu province	Cixi, Zhejiang province	Jingzhou, Hubei province
pH (H ₂ O)	6.63	5.95	8.25	6.70
OM ^a (%)	2.67	1.52	2.48	1.98
CEC ^b (cmol kg ⁻¹)	14.09	7.11	16.1	13.9
clay (%)	38.7	33.5	24.3	33.0
silt (%)	50.4	49.8	71.1	51.2
sand (%)	10.9	16.7	4.6	15.8
texture (%)				
<0.01 mm	67.4	60.7	64.7	67.4
0.01–0.09 mm	28.3	32.6	34.5	28.3
>0.09 mm	4.3	6.7	0.8	4.3
total N (%)	0.24	0.08	1.03	0.12
P (mg kg ⁻¹)	21.25	7.65	15.37	10.25
K (g kg ⁻¹)	13.47	10.7	22.9	5.22

^aOrganic matter. ^bCation exchange capacity.

province), and yellow paddy soil (H, GB/T-A2111511, Jingzhou, Hubei province), respectively. The soil samples were taken from the surface zone (0–15 cm depth) in rice fields in Fujian, Jiangsu, Zhejiang, and Hubei provinces, China. Their basic physicochemical characteristics were determined according to methods previously reported by Gee et al. and are listed in Table 1.²⁰

Degradation Experiments in Soils. To study the behavior and degradation of IPP in anaerobic soils, IPP was sprayed into the test soils to give a final concentration of 20 mg kg⁻¹ of soil and thoroughly mixed. The soil moisture content was adjusted to about 60% of the maximum water-holding capacity by adding Milli-Q (MQ) water. The incubation

temperature was controlled at 25 ± 1 °C in an anaerobic incubator. Ten grams of soil was sampled from the flask at different time intervals (0, 5, 10, 20, 30, 45, 60, 75, and 100 days after treatment, DAT) for determining the concentration of IPP and its metabolites. All experiments were carried out in triplicate.

IPP Extraction. IPP in soils was extracted according to the reported methods.^{21,22} The extraction procedure was employed with each subsequent solvent being less polar. The extraction system was performed as follows in three steps: 0.01 M CaCl₂, dichloromethane, and acetonitrile/water (9:1, v/v). Fifty milliliters of each successive solvent was added and shaken for 1 h. After the first step, the CaCl₂ extract was

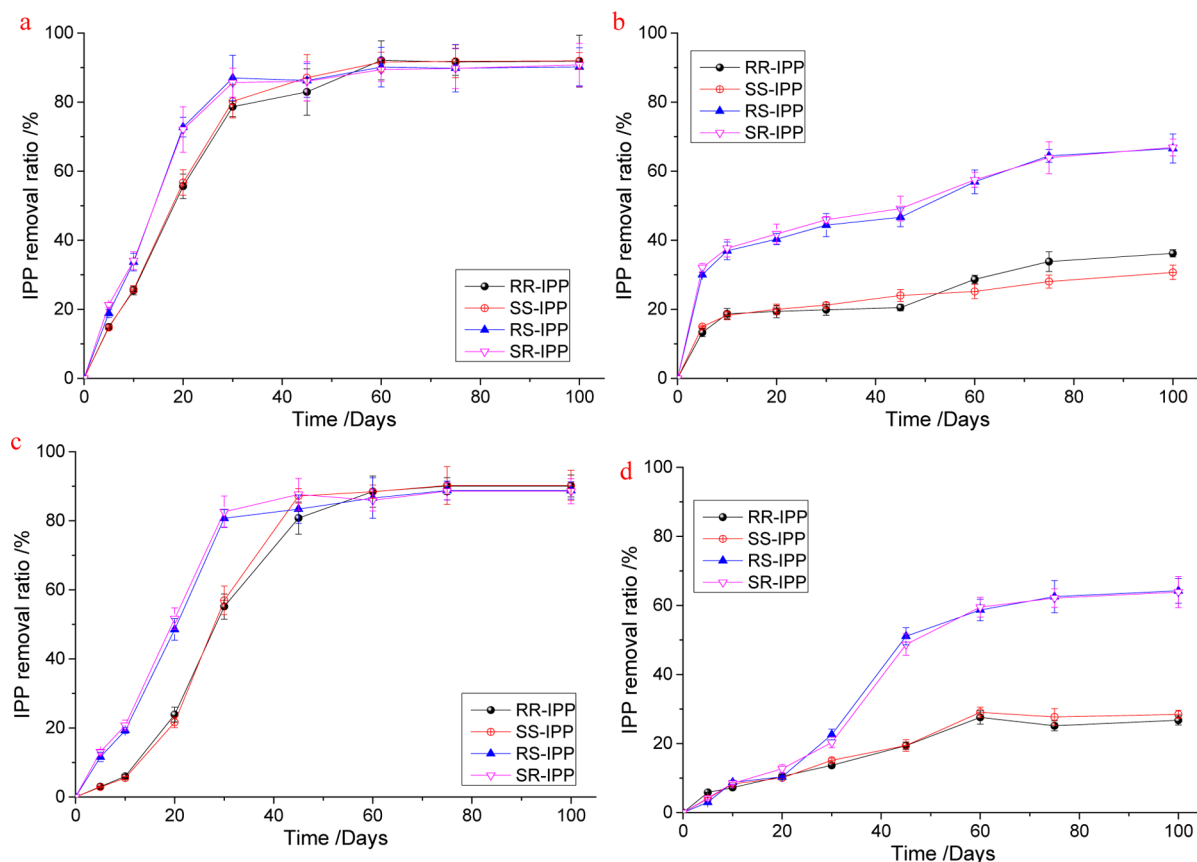


Figure 2. Degradation of RR-IPP, SS-IPP, SR-IPP, and RS-IPP in anaerobic soil: (a) yellow loam soil (F); (b) Huangshi soil (J); (c) paddy field on desalting muddy polder (C); (d) yellow paddy soil (H).

adjusted to pH 3.0 and then extracted with dichloromethane (1:1, v/v) three times. The dichloromethane extract was combined with the other two extracts obtained from the last three extraction steps and concentrated on a vacuum rotary evaporator at 40 °C until dry, and the residue was dissolved in 1 mL of methanol. The overall average recovery of IPP in soils varied from approximately 89.32 to 96.15% in the final extract solution. The relative standard deviations (RSDs) for IPP extraction within each run of soil samples ranged from 2 to 5%, which indicated that the variation between the soil samples was relatively small and within control. These results showed that the method used for IPP extraction and analysis in this study was reproducible and reliable.

Statistical Analysis and Calculation. The aerobic degradation of IPP in soils followed a first-order exponential decay model. The rate constant from the first-order model was used to determine the DT_{50} (half-life value). DT_{50} was calculated by

$$-\ln \frac{C_t}{C_0} = kt \text{ or } C_t = C_0 e^{-kt} \quad (1)$$

where C_0 is the initial concentration of IPP (mg kg^{-1} soil), C_t is the concentration of insecticide at time t , t is the incubation time (days), and k is the degradation rate constant of the insecticide (day^{-1}). DT_{50} and DT_{90} were calculated as $\ln 2/k$ and $\ln 10/k$, respectively.

Analytical Procedures. IPP was determined with high-performance liquid chromatography (HPLC, Agilent 1260, Agilent Technologies, USA); the photodiode array (PDA) detector was operated at 354 nm, with a Daicel Chiralpak IC ($5 \mu\text{m}$, $4.6 \times 250 \text{ mm}$), and the column temperature was 30 °C. The mobile phase was ethanol and pure water (90:10, v/v), and the flow rate was 1.0 mL min^{-1} .

IPP biodegradation intermediates were monitored and analyzed with HPLC (Agilent 1260), 268 nm, C_{18} column ($3.5 \mu\text{m}$, $4.6 \times 250 \text{ mm}$) and 30 °C according to the methods reported by Fu et al.^{5–7} Acetonitrile with 0.1% (v/v) acetic acid (HPLC grade) and a mixture of 0.1% (v/v)

Table 2. Degradation of IPP in Different Anaerobic Soils

soil	IPP	equation	k (day^{-1})	R^2	DT_{50} (days)	DT_{90} (days)
F	RR-IPP	$C_t = 100 e^{-0.0286t}$	0.0286	0.8744	24	81
	SS-IPP	$C_t = 100 e^{-0.0288t}$	0.0288	0.9573	24	80
	RS-IPP	$C_t = 100 e^{-0.0244t}$	0.0244	0.9043	28	94
	SR-IPP	$C_t = 100 e^{-0.0246t}$	0.0246	0.9801	28	94
J	RR-IPP	$C_t = 100 e^{-0.0037t}$	0.0037	0.8660	187	622
	SS-IPP	$C_t = 100 e^{-0.0034t}$	0.0034	0.9493	204	677
	RS-IPP	$C_t = 100 e^{-0.0094t}$	0.0094	0.8863	74	245
	SR-IPP	$C_t = 100 e^{-0.0092t}$	0.0092	0.8760	75	250
H	RR-IPP	$C_t = 100 e^{-0.0033t}$	0.0033	0.8860	210	698
	SS-IPP	$C_t = 100 e^{-0.0036t}$	0.0036	0.8953	193	640
	RS-IPP	$C_t = 100 e^{-0.0122t}$	0.0122	0.9202	57	189
	SR-IPP	$C_t = 100 e^{-0.0121t}$	0.0121	0.9218	57	190
C	RR-IPP	$C_t = 100 e^{-0.0286t}$	0.0286	0.9055	24	81
	SS-IPP	$C_t = 100 e^{-0.0291t}$	0.0291	0.9634	24	79
	RS-IPP	$C_t = 100 e^{-0.0245t}$	0.0245	0.9302	28	94
	SR-IPP	$C_t = 100 e^{-0.0241t}$	0.0241	0.8962	29	96

acetic acid in water (HPLC grade) was at a linear gradient program (minutes/% acetonitrile: 0/15; 7/15; 20/35; 40/100; 45/100; 50/15; 60/15). The flow rate was 1.0 mL min^{-1} .

LC-MS/MS analysis was conducted using a Dionex U3000 HPLC system coupled with a Bruker maXis 4G ion trap mass spectrometer with electrospray ionization source (ESI). LC separation conditions were accordance with those used for HPLC analysis. The ion source

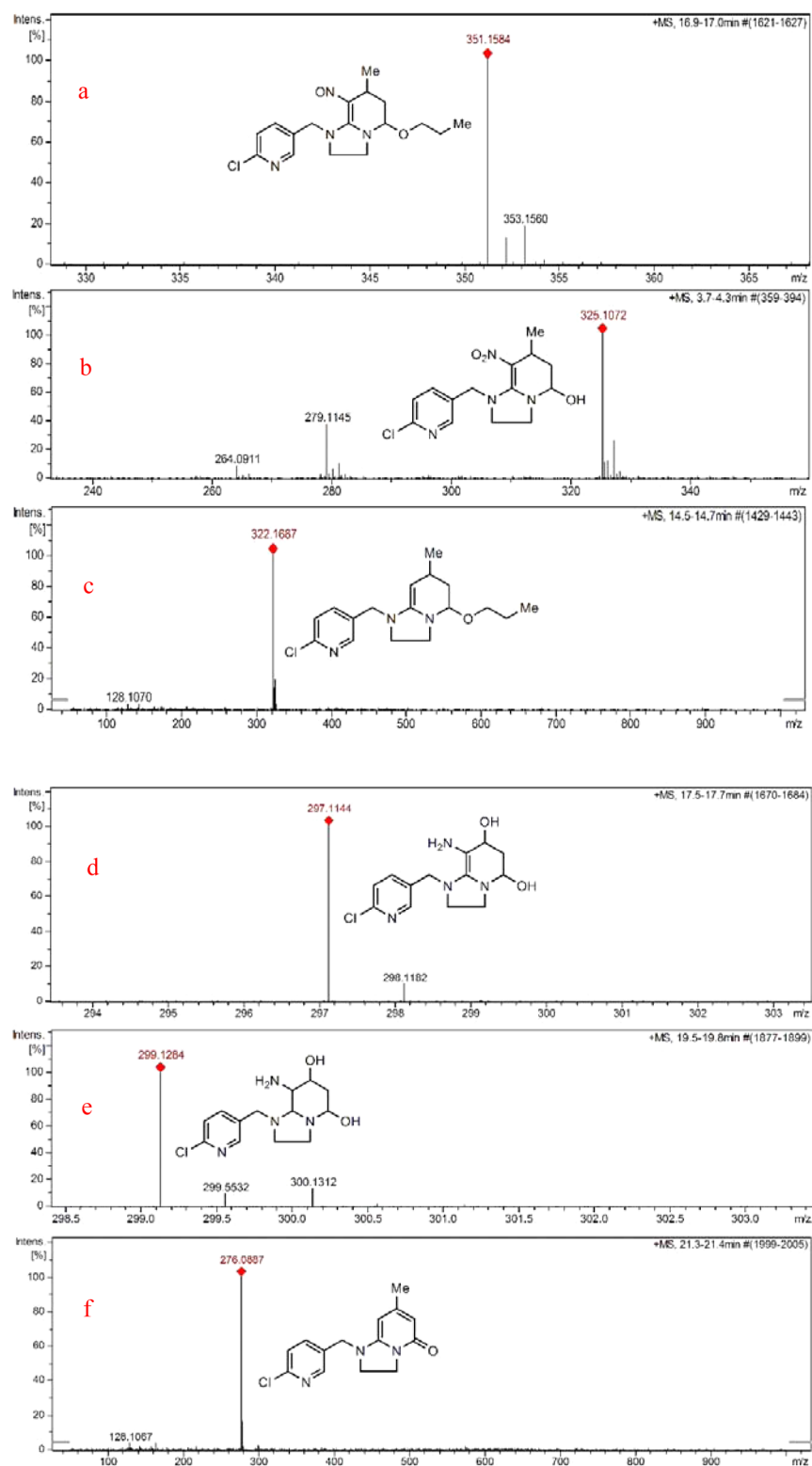


Figure 3. Mass spectra of metabolites (M1, M2, M3, M4, M5, and M6) formed during IPP anaerobic degradation in soils: (a) M1, 1-(6-chloropyridin-3-ylmethyl)-7-methyl-8-nitroso-5-propoxy-1,2,3,5,6,7-hexahydroimidazo[1,2- α]pyridine; (b) M2, 1-((6-chloropyridin-3-yl)methyl)-7-methyl-8-nitro-5-hydroxy-1,2,3,5,6,7-hexahydroimidazo[1,2- α]pyridine; (c) M3, 1-(6-chloropyridin-3-ylmethyl)-7-methyl-5-propoxy-1,2,3,5,6,7-hexahydroimidazo[1,2- α]pyridine; (d) M4, 1-((6-chloropyridin-3-yl)methyl)-5,7-diol-8-amino-1,2,3,5,6,7-hexahydroimidazo[1,2- α]pyridine; (e) M5, 1-((6-chloropyridin-3-yl)methyl)-5,7-diol-8-amino-octahydroimidazo[1,2- α]pyridine; (f) M6, 1-((6-chloropyridin-3-yl)methyl)-2,3-dihydro-5-one-7-methylimidazo[1,2- α]pyridine.

temperature was controlled at 250 °C, and the capillary voltage was −4.5 kV. The analysis mode of ionization was electrospray ionization (ESI, positive). The operation conditions were as follows: collision energy, 10.0 eV; ISCID energy and ion energy, 5.0 eV; dry gas, 6 L min^{−1};

dry temperature, 180 °C; gas pressure, 1.5 bar. The continuous full scanning from *m/z* 50 to 500 Da was performed in positive ion mode.

PCR Amplification of 16S rRNA and Pyrosequencing. The primers 515F (5′-GTGCCAGCMGCCGCGG-3′) and 907R

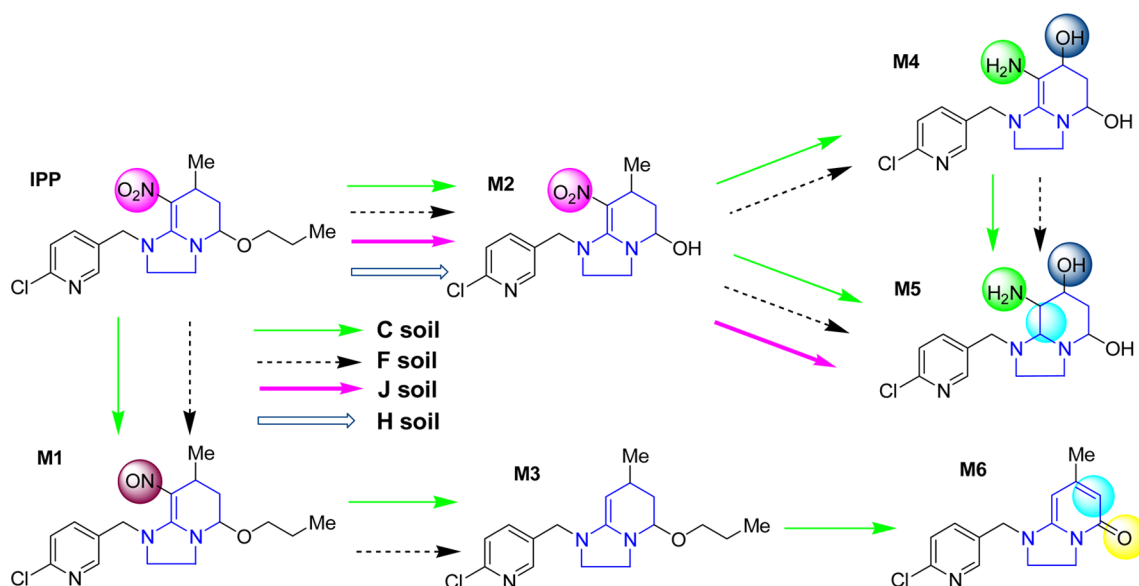


Figure 4. Proposed pathways of IPP degradation in anaerobic soils.

(5'-CCGTCAATTCMTTTRAGTTT-3') were used for amplifying the fragment of the 16S rRNA gene. The PCR reaction program was as follows: 0.2 μ M of each primer and 0.2 mM dNTP, 1.5 mM $MgCl_2$, and 0.2 unit of Taq polymerase. The cycling conditions were 98 $^{\circ}C$ for 30 s, followed by 30 cycles of 98 $^{\circ}C$ for 10 s, 55 $^{\circ}C$ for 20 s, and 72 $^{\circ}C$ for 30 s, with a final extension step at 72 $^{\circ}C$ for 5 min (GeneAmp 9700, ABI, USA). PCR products were purified with the DNA gel recovery kit (Axygen BioScience) and were sent for sequencing service using Miseq sequencing technique (Majorbio Co., Shanghai, China).

Bioinformatic and Statistical Analysis. Totally 240,414 16S rRNA sequence reads were filtered; Trimmomatic was used for denoising and processing. Trimmomatic is a fast, multithreaded command line tool that can be used to trim and crop Illumina (FASTQ) data as well as to remove adapters. The resulting sequences after quality control were analyzed through QIIME. The reads were clustered into operational taxonomic units (OTUs) at 97% sequence similarity using Usearch (version 7.1, <http://drive5.com/uparse/>). OTU representative sequences were aligned against the Greengenes (release 13.5, <http://greengenes.secondgenome.com/>), and chimeric sequences were identified using Mothur (version 1.26). OTU sequences were classified by RDP classifier and QIIME by BLASTING, and the obtained data were used in the subsequent analyses. Community richness was assessed with Chao 1 estimator (<http://www.mothur.org/wiki/Chao>) and ACE estimator (<http://www.mothur.org/wiki/Ace>). Community diversity was estimated with the Shannon index (<http://www.mothur.org/wiki/Shannon>) and the Simpson index (<http://www.mothur.org/wiki/Simpson>).

Statistical analysis was performed in R 2.15.2, using vegan (redundancy analysis (RDA) with significance testing by permutation—ANOVA) and Hmisc packages.

RESULTS AND DISCUSSION

Degradation of IPP in Anaerobic Soils. The results of IPP anaerobic degradation in soils is shown in Figure 2. The removal ratio of all IPP stereoisomers (RR-IPP, SS-IPP, RS-IPP, and SR-IPP) reached >90% at 60 DAT in F and C soils, whereas the RR-IPP and SS-IPP only were <30% in J and H soils. In J and H soils, the removal of RS-IPP and SR-IPP was greater than that of RR-IPP and SS-IPP, and RR-IPP and SS-IPP were hard to degrade in these two soils. The results showed that IPP enantiomer degradation rate differed in different soils and that the IPP degradation rate was higher in F and C soils. IPP, especially RR-IPP and SS-IPP, were relatively hard to degrade in

J and H soils. Degradation of IPP in anaerobic soils followed a first-order exponential decay model. The first-order exponential equation, k , DT_{50} , and DT_{90} are listed in Table 2. The IPP degradation rate was the same in F and C soils, and a similar degradation rate was observed in J and H soils. DT_{50} values of RR-IPP, SS-IPP, RS-IPP, and SR-IPP in F soil were 24, 24, 28, and 28 days, respectively.

It has been reported that greater total carbon (TC) contributes to a larger organic chemical biodegradation rate because the increased carbon content can enhance microorganisms that are responsible for degrading organic pollutants.²³ In this study, the TC content in F and C soils was higher than that in J and H soils. Moreover, the pH value of soil also affects the soil microbial and enzyme activity, which acted as the key important role during IPP degradation process. The IPP degradation rate in F and C soils was higher than that in J and H soils, the reason being that the pH value in F and C soil was appropriate for microbial growth and activity. The lower pH value in J and H soils lead to the slower degradation rate. These results illustrate that the soils with rich OM and neutral pH lead to a greater IPP degradation rate, because these provide suitable conditions for IPP-degrading bacterial growth and biodegradation.

Identification of Metabolites of IPP. During the degradation of IPP in anaerobic soils, six degradation metabolites were detected by HPLC analysis with retention times of 16.9 min (M1), 4.1 min (M2), 14.6 min (M3), 17.6 min (M4), 19.7 min (M5), and 21.3 min (M6). These intermediates occurred with the decrease of IPP. All six intermediates were determined in C soil, and M1, M2, M3, M4, and M5 appeared during IPP anaerobic degradation in F soil. M2 and M5 were determined in J soil, whereas M2 was found in H soil. Six degradation intermediates of IPP were analyzed and identified by high-performance chromatography-time-of flight mass spectrometry (LC-MS) and LC-MS/MS.

The ion fragments of IPP were at m/z 367.1500 ($C_{17}H_{23}ClN_4O_3$) $[M + H]^+$ and m/z 321.1578, and the ion fragment of m/z 367.1500 includes daughter ions of 306.1368 (100), 308.4442 (15), and 137.1069 (62), which were in accordance with the structure of standard IPP.^{5–7,14}

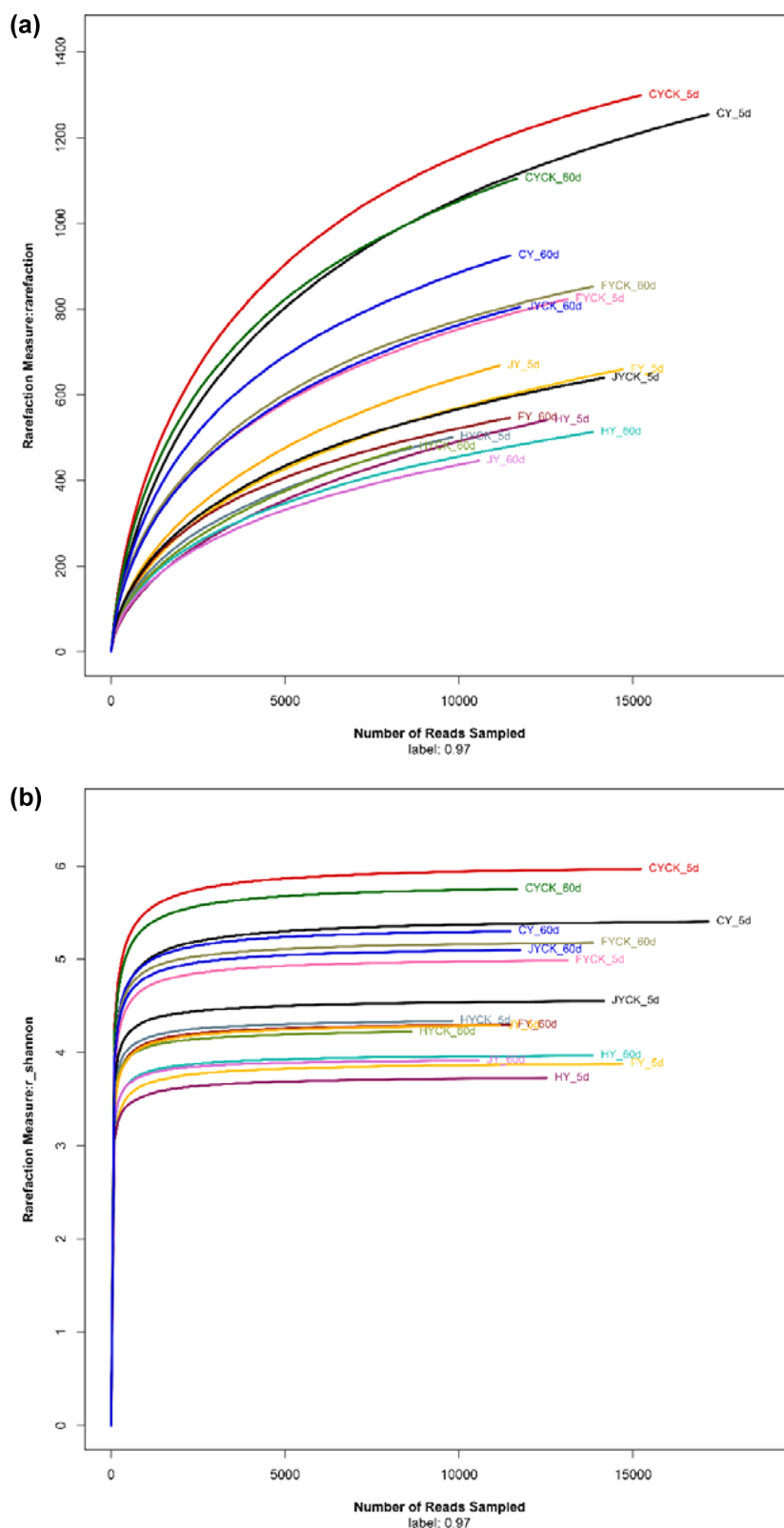


Figure 5. Bacterial diversity comparison with rarefaction curves (a) and Shannon–Wiener curves (b) in different soils at 5 and 60 DAT: (CK_5d and CK_60d) control experiment without IPP spray at 5 and 60 DAT; (CY_5d and CY_60d) C soil with IPP spray at 5 and 60 DAT; (JY_5d and JY_60d) J soil with IPP spray at 5 and 60 DAT; (HY_5d and HY_60d) H soil with IPP spray at 5 and 60 DAT; (JY_5d and JY_60d) J soil with IPP spray at 5 and 60 DAT.

M1 showed m/z 351.1583, and the daughter ion showed m/z 278.1039; the daughter ion should be formed by the loss of a propoxyl group from the parent compound IPP.

M1 was attributed to loss of oxygen from the nitro group and was identified as 1-(6-chloropyridin-3-ylmethyl)-7-methyl-8-nitroso-5-propoxy-1,2,3,5,6,7-hexahydroimidazo[1,2- α]pyridine

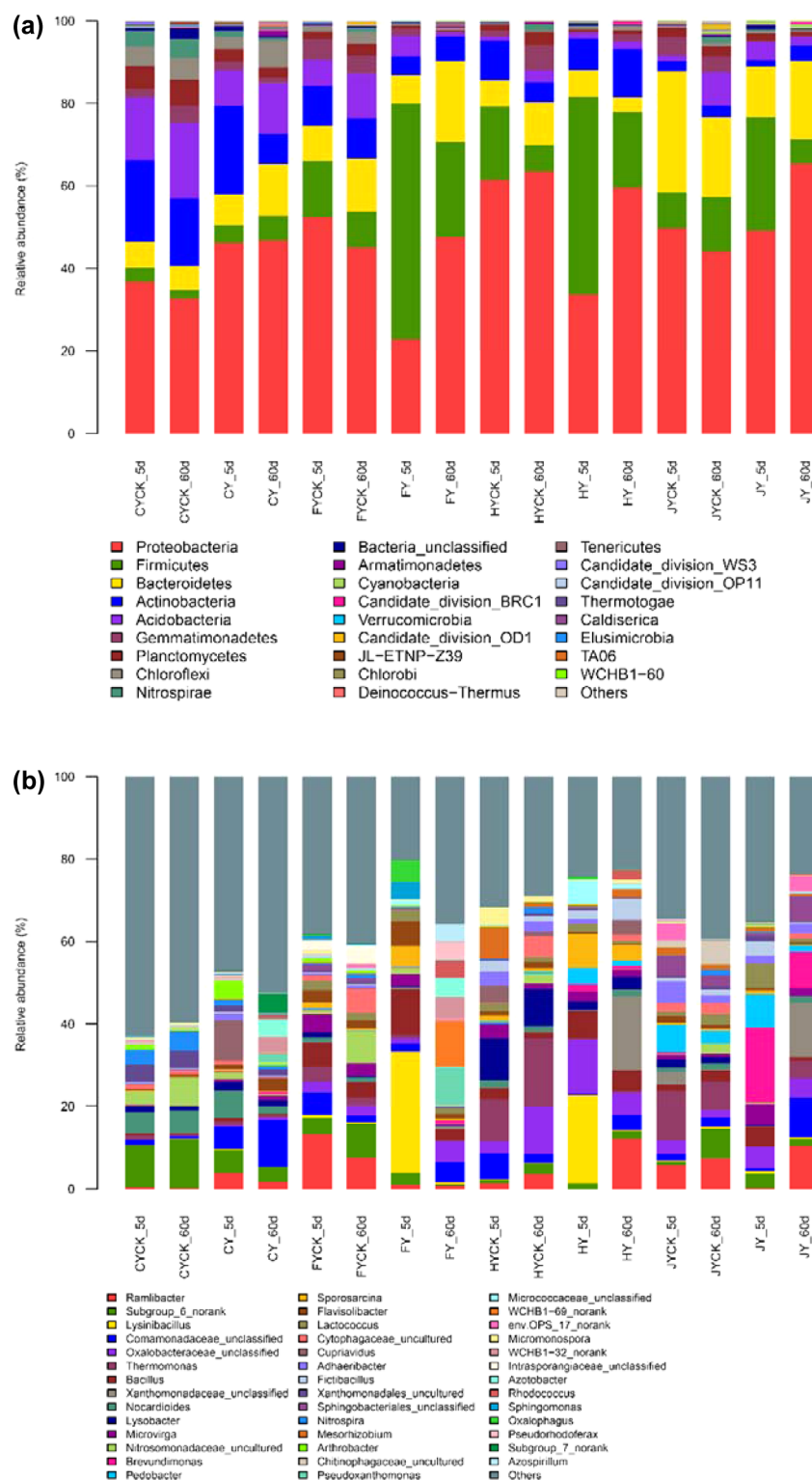


Figure 6. Bacterial composition of the different communities in anaerobic soils: (a) % of relative read abundance of bacterial phyla within each community; (b) % of relative read abundance of bacterial genus within each community.

(Figure 3a). Metabolite M2 was identified as 1-((6-chloropyridin-3-yl)methyl)-7-methyl-8-nitro-5-hydroxy-1,2,3,5,6,7-hexahydroimidazo[1,2- α]pyridine according to its LC-MS/MS and MS² spectra (Figure 3b). The ion fragment of M2 was at m/z 325.1072 $[M + H]^+$, which indicated that M2 was generated through hydrolysis of the propoxyl group of IPP.

The intermediate M3 was at m/z 322.1687 ($C_{17}H_{24}ClN_3O$) $[M + H]^+$, and its daughter ions were m/z 322.1687 and 324.1672. M3 likely corresponded to the loss of the group of 8-nitroso on M1 and was identified as 1-(6-chloropyridin-3-ylmethyl)-7-methyl-5-propoxy-1,2,3,5,6,7-hexahydroimidazo[1,2- α]pyridine, which was in accordance with previous reports (Figure 3c).^{7,14} Figure 3d shows that the m/z of metabolite M4

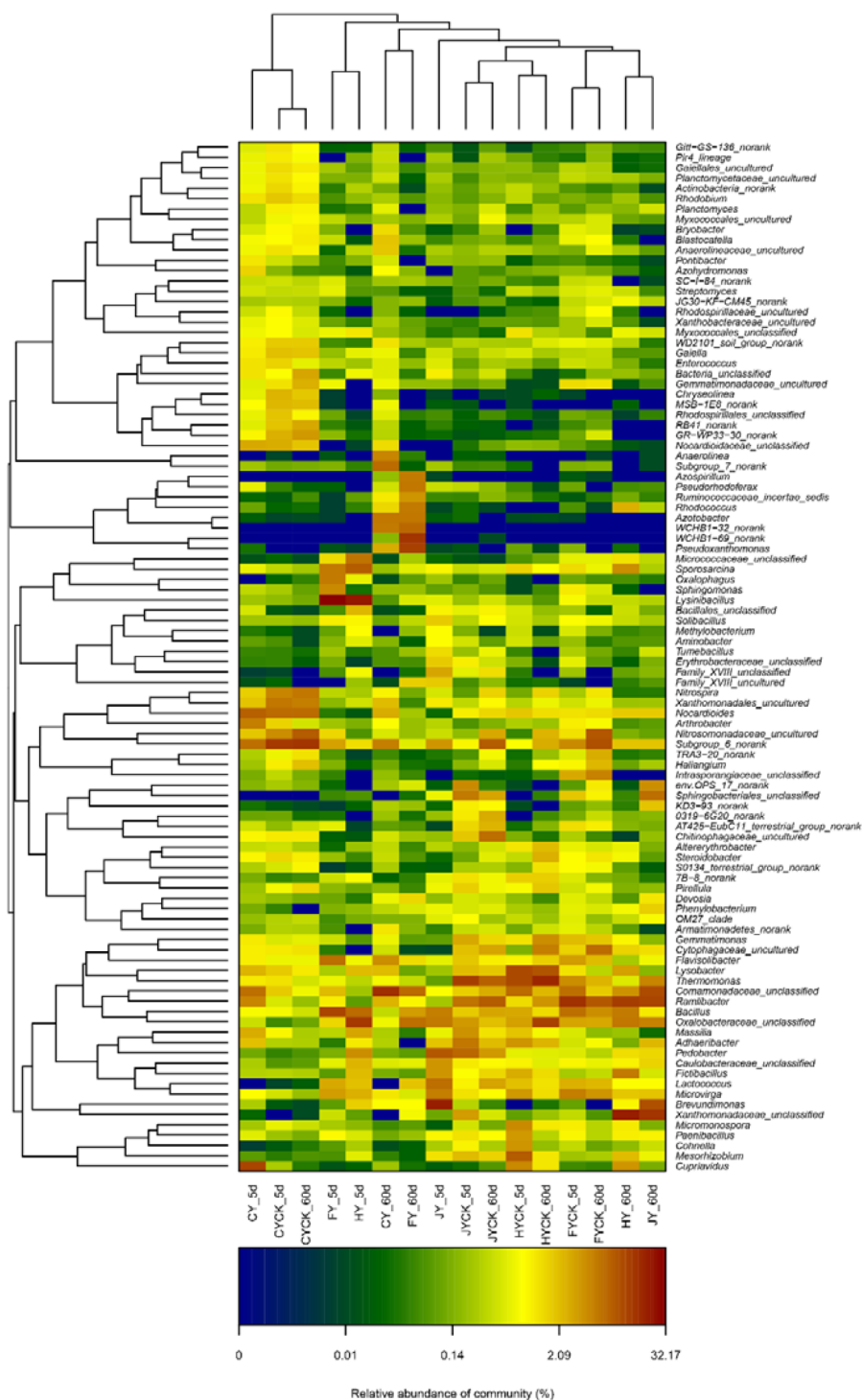


Figure 7. Distribution heatmap of microbial genus arranged by hierarchical clustering of S1 and S2 soils with different treatments.

was 297.1144, which should be the transformation of the group of 8-nitroso on M2 to the 8-amino group, and the nitroso group on M1 transformed to hydroxyl. On the basis of these characteristics, M4 was preliminarily identified as 1-((6-chloropyridin-3-yl)methyl)-5,7-diol-8-amino-1,2,3,5,6,7-hexahydroimidazo[1,2- α]pyridine.

The intermediate MS, with m/z 299.1284 ($M + H$, Figure 3e), was determined as a derivative of M4 on the basis of the elemental formula fit, adding a mass unit of 2 corresponding to hydrogenation of the $C=C$ double bond. The M5 ions matched the formula $C_{13}H_{18}ClN_3O_3$. Thus, M5 was identified as

1-((6-chloropyridin-3-yl)methyl)-5,7-diol-8-amino-octahydroimidazo[1,2- α]pyridine. M6 appeared after M3 and its m/z was 276.0887 ($M + H$, Figure 3f); the M6 ions matched the formula $C_{14}H_{14}ClN_3O$, and M6 was identified as 1-((6-chloropyridin-3-yl)methyl)-2,3-dihydro-5-one-7-methylimidazo[1,2- α]pyridine.

IPP Anaerobic Degradation Pathway in Soils. In J soil, only two metabolites, M2 and M5, were determined, M2 appearing first and then M5 forming from M2; in H soil, only M2 appeared. Therefore, an anaerobic degradation pathway in J and H soils was proposed (Figure 4). The propyl group of IPP was de-esterified and hydrolyzed to form M2, which was in

accordance with the previous study.^{5–7} The nitro group of M2 could be aminated to form amino, and methyl was hydrolyzed to a hydroxyl group. Thus, M5 was generated through these biocatalyzed reactions.

Therefore, the biodegradation pattern can be described as follows: M1 and M2 are first produced and then increased, and this was then followed by M3, M4, and M5, which appeared at almost the same time. M6 was generated in C soil, and M6 was formed from M3 by the loss of a propyl group on M3. On the basis of the identified metabolites during degradation and their patterns of appearance, the proposed degradation pathway of IPP in soils is as follows (Figure 4): In anaerobic F soil, the nitro group of IPP was reduced to a nitroso group and then formed M1. The nitroso group was eliminated during IPP biodegradation, resulting in the denitration product M3. M2 was determined and generated by the loss of a propyl group from the IPP parent. Subsequently, the nitro group on M2 was aminated to form an amino group, and 7-methyl was transformed to a hydroxyl group; thus, M4 was generated. Both M2 and M4 could be transformed to M5. M6 was generated from M3 only in C soil. On the basis of the identified metabolites during degradation and their patterns of appearance, the proposed degradation pathway of IPP in soils is shown in Figure 4. The metabolites M1, M2, and M3 were in accordance with previous reports.^{5–7} M4 and M5 were first observed and identified during IPP anaerobic degradation in soils. In anaerobic soils, a hydroxyl group appeared during M2 transformation to M4, and the reaction should be catalyzed by methyltransferase from microorganism.

Bacterial Diversity and Community Structure in Anaerobic Soils. The community species diversity is shown in Figure 5a. It can be concluded that the bacterial communities in the CK soils (soils without IPP application) were more diverse than in soils with IPP-spraying, which indicated that IPP can affect soil microbial species diversity and IPP could inhibit some bacteria growth and their activity in soils. Under the same conditions, bacteria in the C and F soils were more diverse than in the J and H soils. The sequence of high-to-low order of organic matter (OM) content was C and F > H and J. OM content affects bacterial growth and activity; this was in accordance with the community diversity. The results of rarefaction analysis (Figure 5a) were also similar to the comparison of Shannon's H' (Figure 5b). Evenness in all samples was close to 0.97 for the 0.03 clustering level, and the highest values were observed in C soil. All of the reads in the microbial community were assigned to bacteria. Proteobacteria was the most abundant phylum in all samples (20.5–62.4%, Figure 6a), Firmicutes was the most abundant in F and H soils with IPP-spraying after 5 DAT (56.2 and 48.3%, respectively). Other major phyla were Bacteroidetes, Actinobacteria, Acidobacteria, Gemmatimonadetes, Planctomycetes, Chloroflexi, and Nitrospirae. The most abundant genera were *Ramlibacter*, *Lysinibacillus*, *Comamonadaceae*, *Oxalobacteraceae*, *Thermomonas*, *Bacillus*, *Nitrosomonadaceae*, and *Sporasarcina* (Figure 6b). The community composition was affected by IPP in anaerobic soils. The relative abundance of *Ramlibacter*, *Thermomonas*, *Nitrosomonadaceae*, and *Nocardioide*s was higher in C soil with IPP spraying than in CK soil, whereas in F soil, the genera *Lysinibacillus*, *Thermomonas*, *Cytophagaceae*, *Sporasarcina*, and *Nitrospira* were stimulated to increase after IPP application. RS-IPP and SR-IPP were quickly degraded in the first 10 days in J soil, whereas in H soil, the two insecticides were quickly degraded between 20 and 40 days (Figure 2b,d). Figure 6 shows that phylum relative abundance of Acidobacteria, Planctomycetes, Cyanobacteria, and Chlorobi in J soil was

higher than in H soil, and *Deinococcus-Thermus* was determined only in J soil. Several studies showed that despite similar microbial composition at the initial stage, microbial response to insecticide application was remarkably different.^{24–27} Insecticide-degrading bacteria rapidly increased in the soils after insecticide application. Itoh et al. reported that *O,O*-dimethyl *O*-(3-methyl-*p*-nitrophenyl) phosphorothioate (MEP) degrading microbes increased rapidly after MEP application. Microbial response to MEP application was different, and MEP-degrading *Burkholderia* bacteria are predominant in soils.²⁴ Formesafen and its residues also affect soil microbial activity and soil microbial communities.²⁷ The clustered heatmap analysis based on the bacterial community profiles at the genus level disclosed that the bacterial communities in anaerobic soils after spray IPP shared higher similarity (Figure 7). The bacterial profile in anaerobic soils was distant from that of anaerobic soils after IPP-spraying.

Conclusions. The results in this study show that IPP anaerobic degradation rate is different in four different kinds of soil. Soils' physical–chemical characteristics strongly influenced IPP degradation rate. The metabolites of IPP degradation in soils were identified, and anaerobic degradation pathways were proposed, which presents novel biodegradation pathway of IPP in soils. The determination of new metabolites is very important for better understanding of the mechanism and pathway of IPP biodegradation in anaerobic soils. The bacterial communities in the CK soils were more diverse than in soils with IPP-spraying. Both the rarefaction curves and Shannon–Wiener diversity index in anaerobic soils showed significant difference after IPP application, and the community composition also differed at both phyla and genus levels. The results suggest that application of IPP may change the soil microbial community; IPP-degrading bacteria increased quickly after IPP application in soils.

AUTHOR INFORMATION

Corresponding Authors

* (Z.C.) Phone: 86-519-86330165. Fax: 86-519-86330165. E-mail: zhqcai@cczu.edu.cn.

* (G.Y.) Phone: 86-519-86330194. Fax: 86-519-86330194. E-mail: yguanghua@cczu.edu.cn.

Funding

The research was financially funded by grants from the National Natural Science Foundation of China (NSFC) (Project 11275033) and the Talent Introduction Foundation of Changzhou University (No. ZMF13020003).

Notes

The authors declare no competing financial interest.

REFERENCES

- (1) Liu, W.; Gan, J.; Schlenk, D.; Jury, W. A. Enantioselectivity in environmental safety of current chiral insecticides. *Proc. Natl. Acad. Sci. U. S. A.* **2005**, *102* (3), 701–706.
- (2) Liu, W. P.; Gan, J. Y.; Lee, S.; Werner, I. Isomer selectivity in aquatic toxicity and biodegradation of bifenthrin and permethrin. *Environ. Toxicol. Chem.* **2005**, *24*, 1861–1866.
- (3) Liu, W. P.; Lin, K. D.; Gan, J. Y. Separation and aquatic toxicity of enantiomers of the organophosphorus insecticide trichloronate. *Chirality* **2006**, *18*, 713–716.
- (4) Li, J.; Zhang, J.; Li, C.; Wang, W.; Yang, Z.; Wang, H.; Gan, J.; Ye, Q.; Xu, X.; Li, Z. Stereoisomeric isolation and stereoselective fate of insecticide Paichongding in flooded paddy soils. *Environ. Sci. Technol.* **2013**, *47*, 12768–12774.
- (5) Fu, Q.; Wang, Y.; Zhang, J.; Zhang, H.; Bai, C.; Li, J.; Wang, W.; Wang, H.; Ye, Q.; Li, Z. Soil microbial effects on the stereoselective mineralization, extractable residue, bound residue and metabolism of a

novel chiral cis neonicotinoid, paichongding. *J. Agric. Food Chem.* **2013**, 61, 7689–7695.

(6) Fu, Q.; Zhang, J.; Xu, X.; Wang, H.; Wang, W.; Ye, Q.; Li, Z. Diastereoselective metabolism of a novel cis-nitromethylene neonicotinoid paichongding in aerobic soils. *Environ. Sci. Technol.* **2013**, 47, 10389–10396.

(7) Cai, Z.; Zhang, W.; Li, S.; Ma, J.; Wang, J.; Zhao, X. Microbial degradation mechanism and pathway of the novel insecticide Paichongding by a newly isolated *Sphingobacterium* sp. P1-3 from soil. *J. Agric. Food Chem.* **2015**, 63, 3823–3829.

(8) Wang, H.; Yang, Z.; Liu, R.; Fu, Q.; Zhang, S.; Cai, Z.; Li, J.; Zhao, X.; Ye, Q.; Wang, W.; Li, Z. Stereoselective uptake and distribution of the chiral neonicotinoid insecticide, Paichongding, in Chinese pak choi (*Brassica campestris* ssp. *chinensis*). *J. Hazard. Mater.* **2013**, 262, 862–869.

(9) Kalyani, S. S.; Sharma, J.; Dureja, P.; Singh, S.; Lata. Influence of endosulfan on microbial biomass and soil enzymatic activities of a tropical Alfisol. *Bull. Environ. Contam. Toxicol.* **2010**, 84, 351–356.

(10) Defo, M. A.; Njine, T.; Nola, M.; Beboua, F. S. Microcosm study of the long term effect of endosulfan on enzyme and microbial activities on two agricultural soils of Yaounde-Cameroon. *Afr. J. Agric. Res.* **2011**, 6, 2039–2050.

(11) Cycon, M.; Markowicz, A.; Borymski, S.; Wojcik, M.; Piotrowska-Seget, Z. Imidacloprid induces changes in the structure, genetic diversity and catabolic activity of soil microbial communities. *J. Environ. Manage.* **2013**, 131, 55–65.

(12) Nasreen, C.; Jaffer Mohiddin, G.; Srinivasulu, M.; Rekha Padmini, A.; Ramanamma, P.; Rangaswamy, V. Interaction effects of insecticides on enzyme activities in black clay soil from groundnut (*Arachis hypogaea* L.) fields. *Environ. Res. Eng. Manage.* **2012**, 2 (60), 21–28.

(13) Gundi, V.; Viswanath, B.; Chandra, M. S.; Kumar, V. N.; Reddy, B. R. Activities of cellulase and amylase in soils as influenced by insecticide interactions. *Ecotoxicol. Environ. Saf.* **2007**, 68, 278–285.

(14) Zhao, X.; Shao, X.; Zou, Z.; Xu, X. Photodegradation of novel nitromethylene neonicotinoids with tetrahydropyridine-fixed cis configuration in aqueous solution. *J. Agric. Food Chem.* **2010**, 58, 2746–2754.

(15) Shao, X.; Zhang, W.; Peng, Y.; Li, Z.; Tian, Z.; Qian, X. cis-Nitromethylene neonicotinoids as new nicotinic family: synthesis, structural diversity, and insecticidal evaluation of hexahydroimidazo-[1,2- α]pyridine. *Bioorg. Med. Chem. Lett.* **2008**, 18, 6513–6516.

(16) Tian, Z.; Shao, X.; Li, Z.; Qian, X.; Huang, Q. Synthesis, insecticidal activity, and QSAR of novel nitromethylene neonicotinoids with tetrahydropyridine fixed cis configuration and exo-ring ether modification. *J. Agric. Food Chem.* **2007**, 55, 2288–2292.

(17) Fu, Q.; Wang, W.; Wang, H.; Zhang, J.; Shen, J.; Li, Z.; Ye, Q. Stereoselective fate kinetics of chiral neonicotinoid insecticide paichongding in aerobic soils. *Chemosphere* **2015**, 138, 170–175.

(18) Shao, X.; Fu, H.; Xu, X.; Liu, Z.; Li, Z.; Qian, X. Divalent and oxabridged neonicotinoids constructed by dialdehydes and nitromethylene analogues of imidacloprid: design, synthesis, crystal structure, and insecticidal activities. *J. Agric. Food Chem.* **2010**, 58, 2696–2702.

(19) Shao, X.; Lee, P. W.; Liu, Z.; Xu, X.; Li, Z.; Qian, X. cis-Configuration: a new tactic/rationale for neonicotinoid molecular design. *J. Agric. Food Chem.* **2011**, 59, 2943–2949.

(20) Gee, G. W.; Bauder, J. W. Particle-size analysis. In *Methods of Soil Analysis, Part 1, Physical and Mineralogical Methods*; Klute, A., Ed.; Soil Science Society of America: Madison, WI, USA, 1986; pp 383–412.

(21) Cai, Z.; Wang, H.; Shi, S.; Wang, W.; Chen, Q.; Zhao, X.; Ye, Q. Aerobic biodegradation kinetics and pathway of the novel herbicide ZJ0273 in soils. *Eur. J. Soil Sci.* **2013**, 64, 37–46.

(22) Mordaunt, C. J.; Geva, B.; Jones, K. C.; Semple, K. T. Formation of non-extractable pesticide residues, observations on compound differences, measurement and regulatory issues. *Environ. Pollut.* **2005**, 133 (1), 25–34.

(23) Hirano, T.; Ishida, T.; Kokyo, O.; Sudo, R. Biodegradation of chlordane and hexachlorobenzenes in river sediment. *Chemosphere* **2007**, 67 (3), 428–434.

(24) Itoh, H.; Navarro, R.; Takeshita, K.; Tago, K.; Hayatsu, M.; Hori, T.; Kikuchi, Y. Bacterial population succession and adaptation affected by insecticide application and soil spraying history. *Front. Microbiol.* **2014**, 5, 457.

(25) Fang, H.; Cai, L.; Yang, Y.; Ju, F.; Li, X.; Yu, Y. Metagenomic analysis reveals potential biodegradation pathways of persistent pesticides in fresh water and marine sediments. *Sci. Total Environ.* **2014**, 470–471, 983–992.

(26) Jacobsen, C. S.; Hjelmso, M. H. Agricultural soils, pesticides and microbial diversity. *Curr. Opin. Biotechnol.* **2014**, 27, 15–20.

(27) Wu, X.; Xu, J.; Dong, F.; Liu, X.; Zheng, Y. Responses of soil microbial community to different concentration of fomesafen. *J. Hazard. Mater.* **2014**, 273, 155–164.